Measurements of Z^0 Electroweak Couplings at SLD[*]

Hermann Stängle

University of Massachusetts, Amherst, MA 01003

Representing The SLD Collaboration[**]

Stanford Linear Accelerator Center
Stanford University, Stanford, CA 94309

Abstract

We present a summary of the results of several electroweak measurements performed by the SLD experiment at the Stanford Linear Collider (SLC). Most of these results are preliminary and are based, unless otherwise indicated, on the full 1993-8 data set of approximately 550,000 hadronic decays of Z^0 bosons produced with an average electron beam polarization of 73%.

Invited talk presented at the 14th Rencontres de Physique de la Vallee d'Aoste:

Results and Perspectives in Particle Physics

La Thuile, Italy
February 27–March 4, 2000

1.   Introduction

In the $SU(2)_L \times U(1)$ Standard Model (SM), the vertex factor for the weak neutral current interaction in the $Z^0 \to f\bar{f}$ process is given by:

$$-i\frac{g}{\cos\theta_W}\frac{\gamma^\mu}{2}(v_f - a_f\gamma^5) \tag{1}$$

where v_f and a_f denote the vector and axial-vector couplings:

$$v_f = (c_L^f + c_R^f) = T_f^3 - 2Q_f\sin^2\theta_W, \qquad a_f = (c_L^f - c_R^f) = T_f^3. \tag{2}$$

Here T_f^3 denotes the 3rd component of the fermion weak isospin, Q_f is the electric charge of the fermion, and θ_W represents the electroweak mixing angle.

From combinations of these couplings the Z^0 pole observables A_f and R_f can be formed. A_f represents the extent of parity violation in the coupling of the Z^0 boson to the fermion of type f:

$$A_f = \frac{2v_f a_f}{v_f^2 + a_f^2} = \frac{(c_L^f)^2 - (c_R^f)^2}{(c_L^f)^2 + (c_R^f)^2}, \tag{3}$$

and R_f denotes the fraction of $Z^0 \to f\bar{f}$ events in hadronic Z^0 decays:

$$R_f = \frac{\Gamma(Z^0 \to f\bar{f})}{\Gamma(Z^0 \to \text{hadrons})} \propto (c_L^f)^2 + (c_R^f)^2. \tag{4}$$

The precise experimental determination of A_f and R_f should ultimately verify whether or not the couplings for all generations and weak isospin states are described by the theory isospin assignments and a universal value of $\sin^2\theta_W$.

At Born level, the differential production cross section for $e^+e^- \to Z^0 \to f\bar{f}$ and longitudinally polarized electrons can be written as:

$$\sigma^f(x) = \frac{d\sigma^f}{dx} \propto (1 - A_e P_e)(1 + x^2) + 2A_f(A_e - P_e)x \tag{5}$$

where x denotes the cosine of the polar angle of the outgoing fermion f with respect to the incident electron beam direction, P_e represents the longitudinal polarization of the electron beam, and the positron beam is assumed unpolarized. If one measures the polar angle distribution for a given final state $f\bar{f}$, one can derive the forward-backward production asymmetry:

$$A_{FB}^f(x) = \frac{\sigma^f(x) - \sigma^f(-x)}{\sigma^f(x) + \sigma^f(-x)} = 2A_f\frac{A_e - P_e}{1 - A_e P_e}\frac{x}{1 + x^2} \tag{6}$$

which depends on both the initial and final state coupling parameters as well as on the beam polarization. For zero polarization, one measures the product of couplings $A_e A_f$. If one measures the distributions in equal luminosity samples taken with negative (L)

and positive (R) beam polarization of magnitude P_e, then one can derive the left-right-forward-backward asymmetry:

$$\tilde{A}_{FB}^f(x) = \frac{(\sigma_L^f(x) + \sigma_R^f(-x)) - (\sigma_R^f(x) + \sigma_L^f(-x))}{(\sigma_L^f(x) + \sigma_R^f(-x)) + (\sigma_R^f(x) + \sigma_L^f(-x))} = 2|P_e|A_f \frac{x}{1 + x^2} \qquad (7)$$

for which the dependence on the initial state coupling disappears, allowing a direct measurement of the final state coupling parameter A_f. Thus the presence of electron beam polarization permits unique A_f measurements[1], not only independent of those inferred from the unpolarized forward-backward asymmetry[1] which measures the combination $A_e A_f$, but also with a statistical advantage of $(P_e/A_e)^2 \sim 25$. The initial state coupling is determined most precisely via the left-right cross section asymmetry:

$$A_{LR} = \frac{1}{P_e} \frac{\sigma_L - \sigma_R}{\sigma_L + \sigma_R} = A_e \qquad (8)$$

which yields a very precise measurement of the electroweak mixing angle due to $\delta A_e \sim 8\delta \sin^2 \theta_W$. The measurement and comparison of A_f for the different charged lepton species also provides a direct test of lepton universality.

In addition, precise measurements of A_f and R_f can probe the effect of radiative corrections to the Z^0 propagator or the $Z^0 \to f\bar{f}$ vertex. The radiative corrections depend on the masses of top and Higgs, and precise electroweak measurements can constrain these quantities. The coupling of the Z^0 boson to the b quark is particularly interesting. Physics beyond the SM may couple more strongly to 3rd generation fermions, producing larger deviations in b quark couplings than in other quark couplings. Since $(c_L^b)^2 \sim 30(c_R^b)^2$, R_b has large sensitivity to possible deviations from the predicted left-handed coupling of the Z^0 boson to the b quark, complementary to A_b which has greater sensitivity to the right-handed coupling.

2.   Unique Features of SLD/SLC

The performance of the SLC in the 1997-8 SLD data run has been excellent, with peak luminosities of 3×10^{30} cm^{-2} s^{-1} (i.e. 20,000 Z^0 decays/week). Thus approximately 550,000 Z^0 decays have been collected during the 1993-8 data runs.

A general description of the SLD detector can be found in Ref. [2]. Here we list several of the unique features which allow the SLD experiment to perform many competitive electroweak and heavy flavor measurements:

- A highly longitudinally polarized (average $\sim$73%) electron beam.

- A small and stable beam spot (1.5 μm $\times$ 0.8 μm $\times$ 700 μm) and a high precision 3D CCD-based pixel vertex detector [3] allow the interaction point to be determined to 6 μm $\times$ 6 μm $\times$ 25 μm with an impact parameter resolution of 11 μm $\times$ 23 μm ($r\phi \times rz$) for high momentum tracks.

3

- Good particle identification provided by the Cherenkov Ring Imaging Detector (CRID) [4].

3.   Lepton Coupling Measurements

A.   Left-right Cross Section Asymmetry (A_{LR})

A_{LR} provides a direct measurement of the initial state electron coupling, independent of the final state coupling. No efficiency or acceptance corrections are needed. The final state identification is relatively unsophisticated, and since practically all of the data can be used, A_{LR} can be measured [5] with high statistical precision. In fact, due to the high precision on the polarization measurement, the result is still statistically limited ($\sim 1.3\%$ statistical error compared to $\sim 0.65\%$ systematic error). The precision on A_{LR} demands extensive cross checks to confirm the measurement, and three of the significant more recent checks have been the secondary, independent confirmations of the electron polarization measurement, the verification of the center-of-mass collision energy, and the measurement confirming the absence of positron polarization. The A_{LR} measurement uses all hadronic events and is effectively a counting experiment; $A_{LR} = \frac{1}{P_e} \frac{N_L - N_R}{N_L + N_R}$ where $N_L(N_R)$ denotes the number of Z^0 decays recorded with left (right) electron beam polarization. After applying additional corrections due to γ exchange and γZ^0 interference, we measure $A_{LR}^0 = 0.15108 \pm 0.00218$ and $\sin^2 \theta_W^{eff} = 0.23101 \pm 0.00028$ with the 1992-8 data sample. The A_{LR} measurement provides the most precise single measurement of $\sin^2 \theta_W^{eff}$ presently available.

B. A_{lepton} from $\tilde{A}_{FB}^f$

The lepton couplings A_e, A_μ and A_τ are measured [5] at SLD from leptonic decays of Z^0 bosons making use of the corresponding left-right-forward-backward asymmetry, $\tilde{A}_{FB}^f$, for each lepton type. A_e and A_l (with $l = \mu, \tau$) are extracted simultaneously using a maximum likelihood fit. We obtain $A_e = 0.1558 \pm 0.0064$, $A_\mu = 0.137 \pm 0.016$, and $A_\tau = 0.142 \pm 0.016$. These results are consistent with lepton universality and can be combined to yield $A_{e\mu\tau} = 0.1523 \pm 0.0057$ corresponding to $\sin^2 \theta_W^{eff} = 0.23085 \pm 0.00073$.

4. R_b and R_c Measurements

The R_c [6] and R_b [7] measurements heavily exploit the excellent vertexing capabilities of the SLD via a robust and efficient topological vertex algorithm [8]. Following a standard hadronic event selection, each event is divided into two hemispheres where secondary (and tertiary) vertices are found. After calculating the p_t corrected vertex invariant mass, M_{vtx}, hemispheres are tagged as containing a b quark if $M_{vtx} > 2$ GeV/c^2 and the secondary
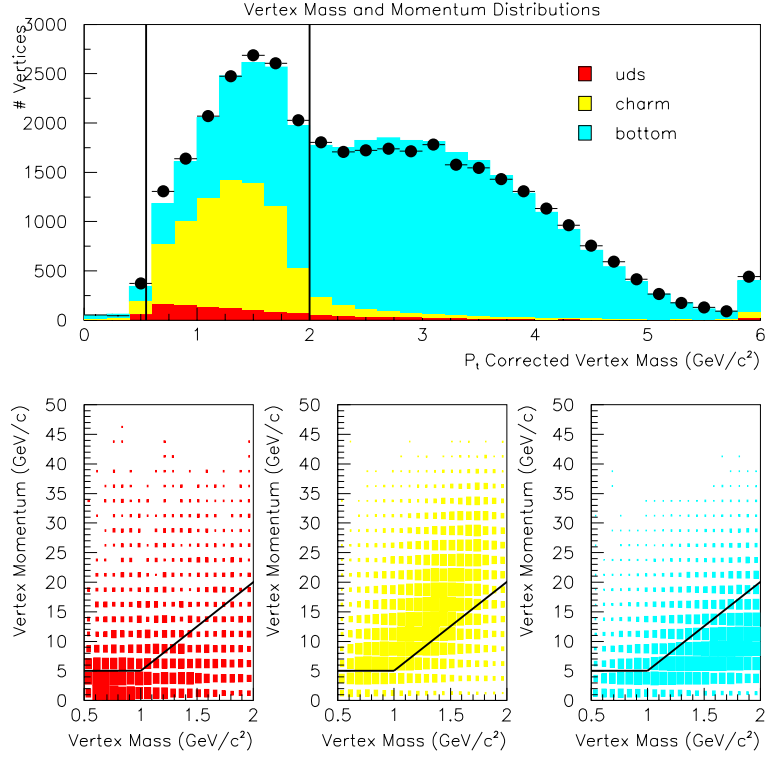
Figure 1: Distributions of (top) M_{vtx} with dots representing the data and (bottom) P_{vtx} vs. M_{vtx} for uds (left) c (middle) and b (right) hemispheres.

vertex is at least 5σ away from the primary vertex. The hemisphere purity for b events is $\sim$98% with $\sim$50% efficiency. Events are selected and tagged as $b\bar{b}$ if at least one of their hemispheres satisfies these conditions. Similarly, an event is tagged as $c\bar{c}$ if there is at least one track with 3D impact parameter more than 3σ from the primary vertex, 0.55 GeV/c^2 < M_{vtx} < 2 GeV/c^2, P_{vtx} > 5 GeV/c and P_{vtx} > $15M_{vtx}c - 10$ GeV/c. The hemisphere purity for c events is $\sim$70% with $\sim$16% efficiency. Figure 1 shows the M_{vtx} and P_{vtx} vs. M_{vtx} distributions for uds, c and b hemispheres. The charm and bottom tagging efficiencies are self-calibrated directly from the experimental data using the single, double and mixed tag rates. The Monte Carlo is used as input for the c and uds efficiencies in the b tag region. Therefore it is important to have high purity in the b tagged event sample in order to reduce the systematic uncertainties due to the modeling of charm production and decay in the simulation. Hemisphere correlations are also derived from the simulation. We measure $R_b = 0.2159 \pm 0.0014(stat.) \pm 0.0014(syst.)$ and $R_c = 0.1685 \pm 0.0047(stat.) \pm 0.0043(syst.)$. Approximately 150,000 hadronic Z^0 decays from the last part of the 1998 run have not yet been included in the R_b result.

5. A_q Measurements

SLD provides several methods to measure the quark couplings A_q, and their statistical and systematic correlations are taken into account in the combinations of their results. All these measurements construct the left-right-forward-backward asymmetries defined previously and use, in different ways, the secondary vertex information. The four different techniques employed to measure A_b make use of the jet charge, the kaon charge, the vertex charge, and the lepton charge to tag the b hemisphere. To determine the c hemisphere, the four A_c measurements employ the kaon or vertex charge, the lepton charge, the soft pion charge or $D^{(*)}$ meson decays reconstructed exclusively. A_s is measured at SLD using identified kaons.

A. A_b with Kaon Tag

The $b \rightarrow c \rightarrow s$ decay chain is exploited in this measurement [9] to tag the sign of the initial b quark. This measurement heavily relies on the good $K^{\pm}$ identification provided by the CRID and the excellent separation between $K^{\pm}$ coming from the secondary vertex and those from the IP. The analyzing power for b events is calibrated from the data. We obtain $A_b = 0.960 \pm 0.040(stat.) \pm 0.069(syst.)$.

B. A_b with Vertex Charge

In this measurement [10], the sum of the charges of tracks attached to the reconstructed vertex is used to tag the initial b quark sign. The analyzing power for b events is calibrated from the data. We measure $A_b = 0.897 \pm 0.027(stat.) \pm 0.034(syst.)$ with the 1996-8 data sample.

C. A_b with Momentum-Weighted Jet Charge

The momentum weighted jet charge [11] is defined as:

$$Q_{diff} = Q_b - Q_{\bar{b}} = - \sum_{tracks} q_i \cdot \text{sgn}(\vec{p}_i \cdot \hat{T})|(\vec{p}_i \cdot \hat{T})|^{\kappa} \tag{9}$$

where $\vec{p}_i$ and q_i denote the ith track momentum and charge, respectively, and $\hat{T}$ represents the direction of the thrust axis. The coefficient κ was chosen to be 0.5 in order to maximize the analyzing power of the tag. Q_{diff} is the difference between the momentum-weighted charges in the two hemispheres. The analyzing power for b events is calibrated from the data. The hemisphere correlation is taken from the simulation. Figure 2 shows the polar angle distributions of the signed thrust axis for left-handed and right-handed electron beams. We measure $A_b = 0.882 \pm 0.020(stat.) \pm 0.029(syst.)$.
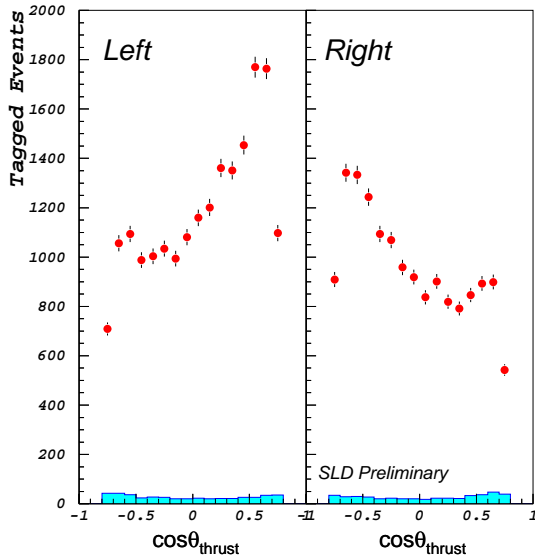
Figure 2: Polar angle distributions of the signed thrust axis for left-handed and right-handed electron beams for the A_b with jet charge analysis. Dots represent the data, and the estimated background is indicated by the shaded histograms.

D. A_b and A_c with Lepton Tag

A_b and A_c can be measured by tagging bottom and charm hadrons using their semileptonic decays [12]. The lepton total and transverse momenta with respect to the nearest jet are employed to calculate the probabilities that the lepton comes from each of the possible physics processes $Z^0 \rightarrow b\bar{b}, b \rightarrow l$; $Z^0 \rightarrow b\bar{b}, \bar{b} \rightarrow \bar{c} \rightarrow l$; $Z^0 \rightarrow b\bar{b}, b \rightarrow \bar{c} \rightarrow l$; $Z^0 \rightarrow c\bar{c}, \bar{c} \rightarrow l$; and background (leptons from light hadron decays, photon conversions, misidentified hadrons). The lepton charge provides quark-antiquark discrimination while the direction of the nearest jet to the lepton approximates the direction of the underlying quark.

Electrons are identified with both calorimeter and CRID information, and this information is incorporated in a neural network trained on Monte Carlo electrons. Muon identification uses information from tracking, the Warm Iron Calorimeter, and the CRID. Both electron and muon identification algorithms have been tested on control samples from data. If an electron is identified in an event, a secondary vertex is required in either hemisphere to reject uds events. If a muon is identified, the vertex mass and the L/D variable, illustrated in Figure 3, are included in the probability function together with the total and transverse lepton momenta. Figure 4 shows how L/D distinguishes between muons from direct and cascade b decays. The topological vertexing algorithm often finds only one vertex for both the B and D decay, thus $L/D < 1$ (> 1) indicates a muon from direct (cascade) b decay. A_b and A_c are determined simultaneously from a maximum likelihood analysis. We measure $A_b = 0.924 \pm 0.032(stat.) \pm 0.026(syst.)$ and $A_c = 0.567 \pm 0.051(stat.) \pm 0.064(syst.)$.
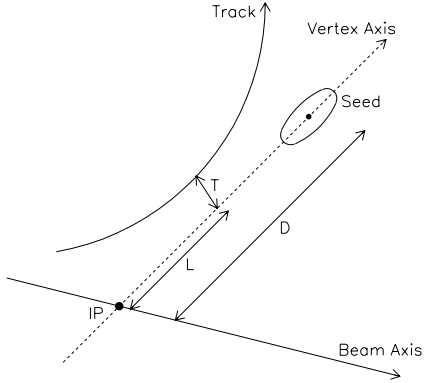
7

Figure 3: Topological track parameters: D is the distance of the secondary vertex seed from the IP, L is the distance from the IP of the projection of the track's point of closest approach on the vertex axis.
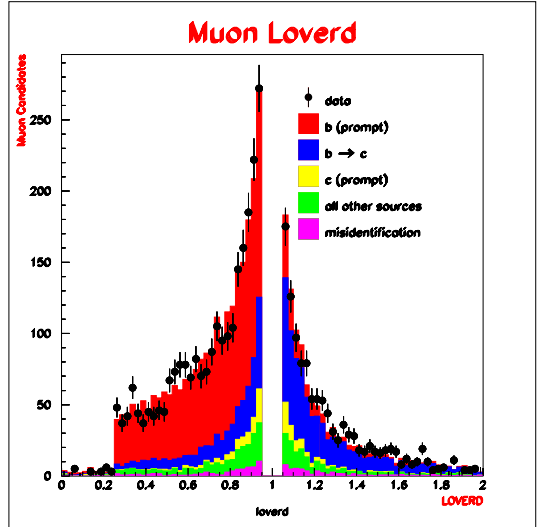

Figure 4: Tails of the L/D distribution for muons in data (dots) and Monte Carlo (histograms).

E. A_c with Exclusive D mesons

This analysis [13] exlusively reconstructs six modes to tag the charm quark: $D^+ \to K^-\pi^+\pi^+$, $D^0 \to K^-\pi^+$, and $D^{*+} \to D^0\pi^+_{soft}$ with D^0 decaying into $K^-\pi^+$, $K^-\pi^+\pi^0$, $K^-\pi^+\pi^+\pi^-$, $K^-l^+\nu_l$ ($l = e$ or μ). Both b and uds backgrounds are rejected with vertex information. The reconstruction efficiency is $\sim 4\%$, however, the high analyzing power and the good determination of the underlying charm quark direction lead to low systematic errors. Figure 5 shows the distribution of the mass difference between D^{*+} and D^0. The background under the signal is estimated from the sidebands. We obtain $A_c = 0.690 \pm 0.042(stat.) \pm 0.022(syst.)$.

F. A_c with Inclusive Soft Pion

In this analysis [13] the charm quark is tagged by the presence of a slow pion from the $D^{*+} \to D^0\pi^+_{soft}$ decay. The soft pion in this decay is produced along the D^{*+} jet direction ($P_T^2 \sim 0$). Figure 6 illustrates the P_T^2 distribution for soft pion tracks. A signal to background ratio of $1 : 2$ is achieved for $P_T^2 < 0.01$ (GeV/c)^2. This method yields $A_c = 0.683 \pm 0.052(stat.) \pm 0.050(syst.)$.

G. A_c with Vertex Charge and Identified Kaons

This analysis [14] uses the charm tag described for the R_c analysis. Furthermore we require at least one hemisphere to pass the charm selection while neither hemisphere passes the
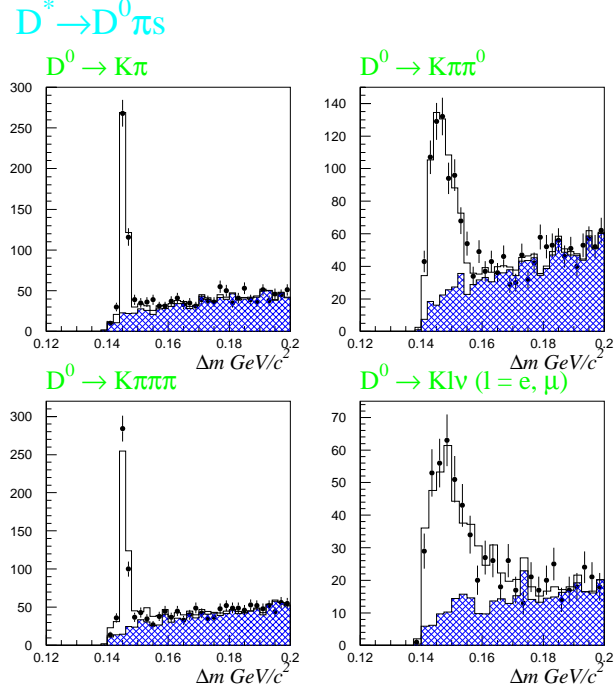
Figure 5: The mass difference distributions for the decay of $D^{*+} \rightarrow D^0 \pi^+_{soft}$ with D^0 decaying into $K^- \pi^+$, $K^- \pi^+ \pi^0$, $K^- \pi^+ \pi^+ \pi^-$, $K^- l^+ \nu_l$ ($l = e$ or μ) in the data (dots) and Monte Carlo (histograms).
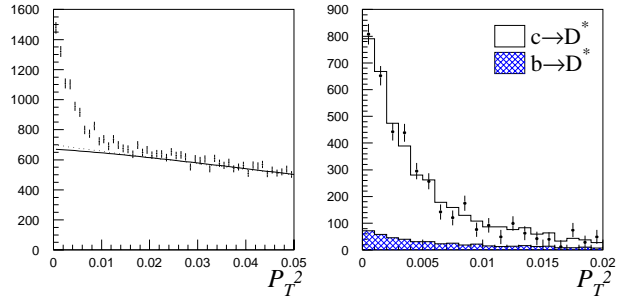

Figure 6: P_T^2 distribution of the soft pion candidates with (left) the full sample and (right) after background subtraction. Dots represent the data.

bottom selection. The sign of the quark charge is determined by the charge of an identified $K^{\pm}$ (or by vertex charge), present in $\sim 25\%$ ($\sim 50\%$) of the selected events with more than 90% correct sign fraction. Figure 7 shows the polar angle distributions of the signed thrust axis for left-handed and right-handed electron beams. The analyzing power for c events is calibrated from the data. We obtain $A_c = 0.603 \pm 0.028(stat.) \pm 0.023(syst.)$.
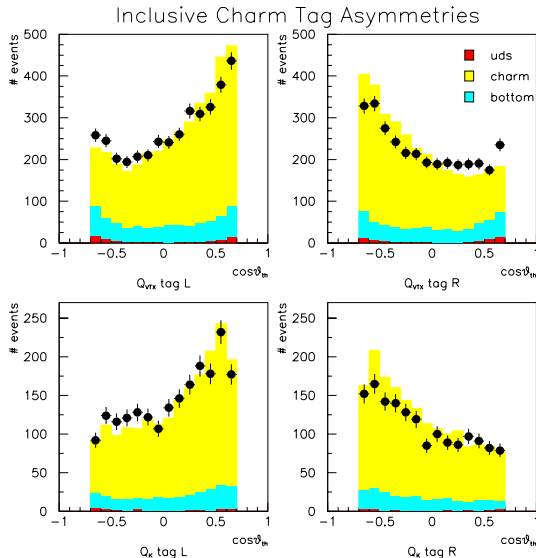

Figure 7: Polar angle distributions of the signed thrust axis for (top) the vertex charge and (bottom) kaon charge channels for data (dots) and Monte Carlo (histograms). The left and right sides show the distributions for the left-handed and right-handed electron beams, respectively.

H. A_s Measurement

At SLD, $s\bar{s}$ events can be identified with relatively high purity due to the good separation of tracks from secondary vertices and the CRID particle identification. In the A_s analysis [15], the charge of an identified $K^{\pm}$ is used to tag the sign of the initial s quark. Information from the vertex detector is used to suppress the background from heavy flavor events. $K^{\pm}$ with $p > 9$ GeV/c and K_s^0 with $p > 5$ GeV/c are selected with 92% and 91% purity, respectively. Each thrust hemisphere of a light flavor tagged event is required to contain at least one identified strange particle. Strange hemispheres are tagged using the highest momentum strange particle present in the hemisphere. A tag is required in both hemispheres and at least one tag must be signed; if both are signed, signs must be opposite. The combined $s\bar{s}$ purity of the K^+K^- and $K^{\pm}K_s^0$ tagging modes is 66%. The initial s quark direction is approximated by the thrust axis in the event, signed to point in the direction of negative strangeness. Figure 8 shows the polar angle distributions for

left-handed and right-handed electron beams. The background from ud events as well as the analyzing power of the method for s events are constrained from the data. We measure $A_s = 0.895 \pm 0.066(stat.) \pm 0.063(syst.)$.
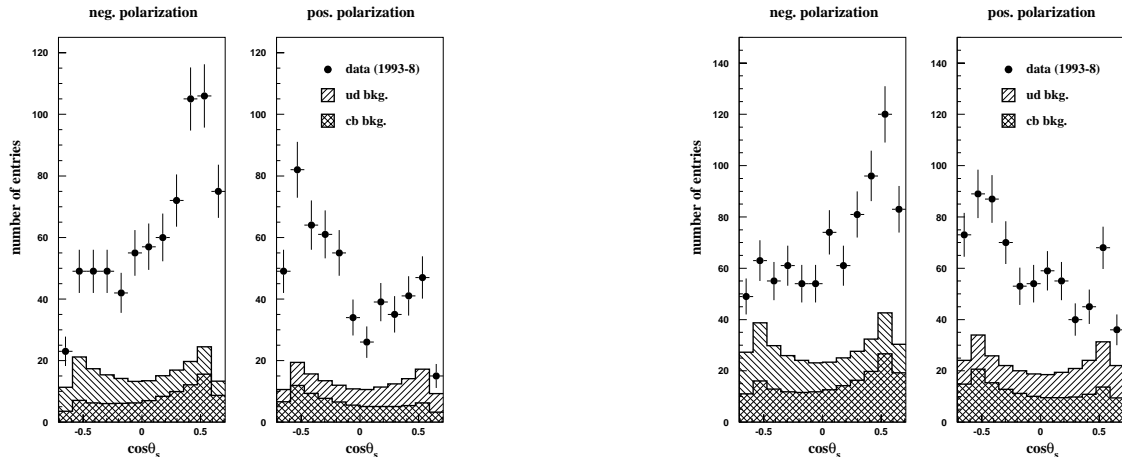

Figure 8: Polar angle distributions of the signed thrust axis for the (left) K^+K^- mode and (right) $K^\pm K^0_s$ mode for left-handed and right-handed electron beams. The dots show data and the background is indicated by the hatched histograms.

6.   Conclusions

We have presented the results of several electroweak measurements performed by the SLD Collaboration. These results are summarized in Table 1. The combined A_{LR} and A_{lepton} SLD measurements yield $\sin^2 \theta_W^{eff} = 0.23099 \pm 0.00026$. The LEP measurements of lepton forward-backward asymmetries and tau polarization have been combined into a LEP lepton based $\sin^2 \theta_W^{eff} = 0.23151 \pm 0.00033$. These results are consistent. Both the R_c and R_b SLD results are in good agreement with the LEP results and the Standard Model prediction. The SLD R_c measurement is the most precise single determination of this variable.

The SLD A_s result is in agreement with LEP results and the Standard model prediction. It is also consistent with previous A_b measurements performed by SLD and LEP, and therefore supports the predicted universality of the Z^0 to down-type quark couplings. The combined SLD A_c measurements give $A_c = 0.634 \pm 0.027$, in agreement with both the corresponding LEP result and the Standard Model prediction. The combined SLD A_b results yield $A_b = 0.905 \pm 0.026$ which is consistent with the Standard Model prediction. The corresponding LEP result is $A_b = 0.881 \pm 0.020$. A combined SLD and LEP average for A_b is about 2.8 standard deviations below the Standard Model prediction.

Table 1: Summary of SLD results of electroweak measurements.

Observable	Preliminary Result
A_{LR}^0	0.15108 ± 0.00218
$\sin^2 \theta_W^{eff}$ (from A_{LR}^0)	0.23101 ± 0.00028
A_e (from $\tilde{A}_{FB}^f$)	0.1558 ± 0.0064
A_μ	0.137 ± 0.016
A_τ	0.142 ± 0.016
$A_{e\mu\tau}$	0.1523 ± 0.0057
$\sin^2 \theta_W^{eff}$ (from A_l)	0.23085 ± 0.00073
$\sin^2 \theta_W^{eff}$ (from A_{LR}^0 and A_l)	0.23099 ± 0.00026
R_c	$0.1685 \pm 0.0047 \pm 0.0043$
R_b	$0.2159 \pm 0.0014 \pm 0.0014$
A_b (kaon tag)	$0.960 \pm 0.040 \pm 0.069$
A_b (vertex charge)	$0.897 \pm 0.027 \pm 0.034$
A_b (jet charge)	$0.882 \pm 0.020 \pm 0.029$
A_b (lepton tag)	$0.924 \pm 0.032 \pm 0.026$
A_b (SLD average)	0.905 ± 0.026
A_c (lepton tag)	$0.567 \pm 0.051 \pm 0.064$
A_c (exclusive D, D^*)	$0.690 \pm 0.042 \pm 0.022$
A_c (inclusive soft pion)	$0.683 \pm 0.052 \pm 0.050$
A_c (vertex charge, kaons)	$0.603 \pm 0.028 \pm 0.023$
A_c (SLD average)	0.634 ± 0.027
A_s	$0.895 \pm 0.066 \pm 0.063$

7.   Acknowledgements

References

[1] The LEP and SLD Electroweak Working Group, CERN-EP/99-15 (1999).

[2] SLD Design Report, SLAC-Report 273 (1984).

[3] C. J. S. Damerell *et al.*, Nucl. Instr. Meth. **A288** 236 (1990).
    C. J. S. Damerell *et al.*, Nucl. Instr. Meth. **A400** 287 (1997).

[4] K. Abe *et al.*, Nucl. Inst. Meth. **A343** 74 (1994).

[5] K. Abe *et al.*, SLAC-PUB-8311, contributed to EPS-HEP (1999).

[6] K. Abe *et al.*, SLAC-PUB-7880, contributed to ICHEP (1998).

[7] K. Abe *et al.*, Phys. Rev. Lett. **80** 660 (1998).

[8] D. Jackson, Nucl. Inst. Meth. **A338** 247 (1997).

[9] K. Abe *et al.*, SLAC-PUB-8200, contributed to EPS-HEP (1999).

[10] K. Abe *et al.*, SLAC-PUB-8201, contributed to EPS-HEP (1999).

[11] K. Abe *et al.*, Phys. Rev. Lett. **81** 942 (1998).
     K. Abe *et al.*, SLD Physics Note 74 (1999).

[12] K. Abe *et al.*, SLAC-PUB-7798 (1999).

[13] K. Abe *et al.*, SLAC-PUB-8195, contributed to EPS-HEP (1999).

[14] K. Abe *et al.*, SLAC-PUB-8199, contributed to EPS-HEP (1999).

[15] K. Abe *et al.*, SLAC-PUB-8154, contributed to EPS-HEP (1999).

**List of Authors

Kenji Abe,[21] Koya Abe,[33] T. Abe,[29] I.Adam,[29] T. Akagi,[29] N. J. Allen,[5]
W.W. Ash,[29] D. Aston,[29] K.G. Baird,[17] C. Baltay,[40] H.R. Band,[39]
M.B. Barakat,[16] O. Bardon,[19] T.L. Barklow,[29] G. L. Bashindzhagyan,[20]
J.M. Bauer,[18] G. Bellodi,[23] R. Ben-David,[40] A.C. Benvenuti,[3] G.M. Bilei,[25]
D. Bisello,[24] G. Blaylock,[17] J.R. Bogart,[29] G.R. Bower,[29] J. E. Brau,[22]
M. Breidenbach,[29] W.M. Bugg,[32] D. Burke,[29] T.H. Burnett,[38] P.N. Burrows,[23]
A. Calcaterra,[12] D. Calloway,[29] B. Camanzi,[11] M. Carpinelli,[26] R. Cassell,[29]
R. Castaldi,[26] A. Castro,[24] M. Cavalli-Sforza,[35] A. Chou,[29] E. Church,[38]
H.O. Cohn,[32] J.A. Coller,[6] M.R. Convery,[29] V. Cook,[38] R. Cotton,[5]
R.F. Cowan,[19] D.G. Coyne,[35] G. Crawford,[29] C.J.S. Damerell,[27] M. N. Danielson,[8]
M. Daoudi,[29] N. de Groot,[4] R. Dell'Orso,[25] P.J. Dervan,[5] R. de Sangro,[12]
M. Dima,[10] A. D'Oliveira,[7] D.N. Dong,[19] M. Doser,[29] R. Dubois,[29]
B.I. Eisenstein,[13] V. Eschenburg,[18] E. Etzion,[39] S. Fahey,[8] D. Falciai,[12] C. Fan,[8]
J.P. Fernandez,[35] M.J. Fero,[19] K.Flood,[17] R. Frey,[22] J. Gifford,[36] T. Gillman,[27]
G. Gladding,[13] S. Gonzalez,[19] E. R. Goodman,[8] E.L. Hart,[32] J.L. Harton,[10]
A. Hasan,[5] K. Hasuko,[33] S. J. Hedges,[6] S.S. Hertzbach,[17] M.D. Hildreth,[29]

J. Huber,[22] M.E. Huffer,[29] E.W. Hughes,[29] X.Huynh,[29] H. Hwang,[22]
M. Iwasaki,[22] D. J. Jackson,[27] P. Jacques,[28] J.A. Jaros,[29] Z.Y. Jiang,[29]
A.S. Johnson,[29] J.R. Johnson,[39] R.A. Johnson,[7] T. Junk,[29] R. Kajikawa,[21]
M. Kalelkar,[28] Y. Kamyshkov,[32] H.J. Kang,[28] I. Karliner,[13] H. Kawahara,[29]
Y. D. Kim,[30] M.E. King,[29] R. King,[29] R.R. Kofler,[17] N.M. Krishna,[8]
R.S. Kroeger,[18] M. Langston,[22] A. Lath,[19] D.W.G. Leith,[29] V. Lia,[19] C.Lin,[17]
M.X. Liu,[40] X. Liu,[35] M. Loreti,[24] A. Lu,[34] H.L. Lynch,[29] J. Ma,[38]
G. Mancinelli,[28] S. Manly,[40] G. Mantovani,[25] T.W. Markiewicz,[29]
T. Maruyama,[29] H. Masuda,[29] E. Mazzucato,[11] A.K. McKemey,[5] B.T. Meadows,[7]
G. Menegatti,[11] R. Messner,[29] P.M. Mockett,[38] K.C. Moffeit,[29] T.B. Moore,[40]
M.Morii,[29] D. Muller,[29] V.Murzin,[20] T. Nagamine,[33] S. Narita,[33] U. Nauenberg,[8]
H. Neal,[29] M. Nussbaum,[7] N.Oishi,[21] D. Onoprienko,[32] L.S. Osborne,[19]
R.S. Panvini,[37] C. H. Park,[31] T.J. Pavel,[29] I. Peruzzi,[12] M. Piccolo,[12]
L. Piemontese,[11] K.T. Pitts,[22] R.J. Plano,[28] R. Prepost,[39] C.Y. Prescott,[29]
G.D. Punkar,[29] J. Quigley,[19] B.N. Ratcliff,[29] T.W. Reeves,[37] J. Reidy,[18]
P.L. Reinertsen,[35] P.E. Rensing,[29] L.S. Rochester,[29] P.C. Rowson,[9] J.J. Russell,[29]
O.H. Saxton,[29] T. Schalk,[35] R.H. Schindler,[29] B.A. Schumm,[35] J. Schwiening,[29]
S. Sen,[40] V.V. Serbo,[29] M.H. Shaevitz,[9] J.T. Shank,[6] G. Shapiro,[15]
D.J. Sherden,[29] K. D. Shmakov,[32] C. Simopoulos,[29] N.B. Sinev,[22] S.R. Smith,[29]
M. B. Smy,[10] J.A. Snyder,[40] H. Staengle,[10] A. Stahl,[29] P. Stamer,[28] H. Steiner,[15]
R. Steiner,[1] M.G. Strauss,[17] D. Su,[29] F. Suekane,[33] A. Sugiyama,[21] S. Suzuki,[21]
M. Swartz,[14] A. Szumilo,[38] T. Takahashi,[29] F.E. Taylor,[19] J. Thom,[29]
E. Torrence,[19] N. K. Toumbas,[29] T. Usher,[29] C. Vannini,[26] J. Va'vra,[29]
E. Vella,[29] J.P. Venuti,[37] R. Verdier,[19] P.G. Verdini,[26] D. L. Wagner,[8]
S.R. Wagner,[29] A.P. Waite,[29] S. Walston,[22] J.Wang,[29] S.J. Watts,[5]
A.W. Weidemann,[32] E. R. Weiss,[38] J.S. Whitaker,[6] S.L. White,[32] F.J. Wickens,[27]
B. Williams,[8] D.C. Williams,[19] S.H. Williams,[29] S. Willocq,[17] R.J. Wilson,[10]
W.J. Wisniewski,[29] J. L. Wittlin,[17] M. Woods,[29] G.B. Word,[37] T.R. Wright,[39]
J. Wyss,[24] R.K. Yamamoto,[19] J.M. Yamartino,[19] X. Yang,[22] J. Yashima,[33]
S.J. Yellin,[34] C.C. Young,[29] H. Yuta,[2] G. Zapalac,[39] R.W. Zdarko,[29] J. Zhou.[22]

[1]Adelphi University, Garden City, New York 11530,
[2]Aomori University, Aomori , 030 Japan,
[3]INFN Sezione di Bologna, I-40126, Bologna Italy,
[4]University of Bristol, Bristol, U.K.,
[5]Brunel University, Uxbridge, Middlesex, UB8 3PH United Kingdom,
[6]Boston University, Boston, Massachusetts 02215,
[7]University of Cincinnati, Cincinnati, Ohio 45221,
[8]University of Colorado, Boulder, Colorado 80309,
[9]Columbia University, New York, New York 10533,
[10]Colorado State University, Ft. Collins, Colorado 80523,
[11]INFN Sezione di Ferrara and Universita di Ferrara, I-44100 Ferrara, Italy,
[12]INFN Lab. Nazionali di Frascati, I-00044 Frascati, Italy,
[13]University of Illinois, Urbana, Illinois 61801,

[14] *Johns Hopkins University, Baltimore, MD 21218-2686,*
[15] *Lawrence Berkeley Laboratory, University of California, Berkeley, California 94720,*
[16] *Louisiana Technical University - Ruston,LA 71272,*
[17] *University of Massachusetts, Amherst, Massachusetts 01003,*
[18] *University of Mississippi, University, Mississippi 38677,*
[19] *Massachusetts Institute of Technology, Cambridge, Massachusetts 02139,*
[20] *Institute of Nuclear Physics, Moscow State University, 119899, Moscow Russia,*
[21] *Nagoya University, Chikusa-ku, Nagoya 464 Japan,*
[22] *University of Oregon, Eugene, Oregon 97403,*
[23] *Oxford University, Oxford, OX1 3RH, United Kingdom,*
[24] *INFN Sezione di Padova and Universita di Padova I-35100, Padova, Italy,*
[25] *INFN Sezione di Perugia and Universita di Perugia, I-06100 Perugia, Italy,*
[26] *INFN Sezione di Pisa and Universita di Pisa, I-56010 Pisa, Italy,*
[27] *Rutherford Appleton Laboratory, Chilton, Didcot, Oxon OX11 0QX United Kingdom,*
[28] *Rutgers University, Piscataway, New Jersey 08855,*
[29] *Stanford Linear Accelerator Center, Stanford University, Stanford, California 94309,*
[30] *Sogang University, Seoul, Korea,*
[31] *Soongsil University, Seoul, Korea 156-743,*
[32] *University of Tennessee, Knoxville, Tennessee 37996,*
[33] *Tohoku University, Sendai 980, Japan,*
[34] *University of California at Santa Barbara, Santa Barbara, California 93106,*
[35] *University of California at Santa Cruz, Santa Cruz, California 95064,*
[36] *University of Victoria, Victoria, B.C., Canada, V8W 3P6,*
[37] *Vanderbilt University, Nashville,Tennessee 37235,*
[38] *University of Washington, Seattle, Washington 98105,*
[39] *University of Wisconsin, Madison,Wisconsin 53706,*
[40] *Yale University, New Haven, Connecticut 06511.*